Polymer 51 (2010) 3108–3115

Contents lists available at ScienceDirect

Polymer

journal homepage: www.elsevier.com/locate/polymer

Star-shaped macromolecules with calixarene core and neutral amphiphilic block copolymer arms: New hosts for ions

A.V. Tenkovtsev [a], M.M. Dudkina [a], L.I. Scherbinskaya [a], V. Aseyev [b,*], H. Tenhu [b]

[a] Institute of Macromolecular Compounds, Russian Academy of Sciences, Bolshoy pr. V.O. 31, 199004 St. Petersburg, Russia
[b] Laboratory of Polymer Chemistry, Department of Chemistry, University of Helsinki, P.O. Box 55, FIN-00014 UH, Finland

ARTICLE INFO

Article history:
Received 24 March 2010
Received in revised form
22 April 2010
Accepted 25 April 2010
Available online 23 May 2010

Keywords:
Amphiphilic polymer
Calixarene
Transport properties

ABSTRACT

Two neutral star-shaped polymers with calix[8]arene core and eight amphiphilic alkyloligoethyleneoxide arms have been synthesised using the arm-first approach. One of them has arms with oligoethylene oxide block attached to the calix[8]arene core, whereas the other one has arms where the oligoethylene oxide is the outer block. Both polymers are soluble in most common organic solvents and form true, i.e., molecularly dispersed solutions. In highly dilute aqueous solutions these polymers form loose multimolecular clusters, which do not disintegrate upon further dilution but break in a shear flow. Aggregation of these star polymers in water is investigated using light scattering and the structure of the aggregates is discussed. The ability of the stars to bind a series of metal ions and the effectiveness of these polymers as phase-transfer agents were investigated in respect to their molecular architecture. The performance of the star-shaped polymers was also compared to that of crown ethers.

1. Introduction

Amphiphilic star-shaped block copolymers have attracted much attention because of their ability to self assemble in water into nanosized unimolecular micelles containing hydrophobic cores surrounded by hydrophilic shells. Star-shaped block copolymers with hydrophobic inner blocks typically are directly soluble in water. This property makes them more attractive, in comparison with amphiphilic linear block copolymers having the same chemical composition, because their solubilisation does not necessarily require a transfer from an organic solvent into an aqueous medium. As has been demonstrated, star-block copolymers are capable to form supramolecular structures of various morphologies, e.g., single and multi core micelles or worm-like micelles [1]. These structures are of great interest for medical applications such as micelle-assisted drug delivery [2]. Star polymers synthesized using multifunctional calixarene initiators have additional fascinating features. The macro cyclic core composed of benzene rings has a structure, which allows its complexation with low molecular weight compounds [3], molecular recognition, as well as the preparation of supramolecular assemblies using macrocycles as building blocks [4–6]. Synthesis of calixarenes and functionalizing of the lower and the upper rim of calixarenes is easy and have resulted in a variety of derivatives [7,8]. Effective encapsulation (i.e., binding to the calixarene core) of small molecules poorly soluble in water (drugs, dyes, flavors, fragrances *etc.*) is necessary to protect them from hydrolytic and oxidative degradation [9,10]. The calixarene core can also be used as a molecular container for photoactive substances. In all these cases, the formation of a complex with calixarene results in a change in the spectral characteristics of the substance owing to the redistribution of the electron density [11].

There are two basic approaches to the synthesis of the star-shaped macromolecules: the arm-first and the core-first techniques. The arm-first technique involves the synthesis of the preformed arms that are bound together with multifunctional linking agents [12–15]. The core-first approach is preferable in the case of the stars synthesized using calixarene-based initiators especially in a combination with the living ionic or controlled radical polymerization. Kennedy and co-workers introduced a calix[8]arene-based initiator in the living cationic polymerization of isobutylene [16,17]. Later Sawamoto et al. [18] and Gnanou et al. [19–21] used functionalized calix[*n*]arenes as ATRP initiators in polymerization of styrene, methyl methacrylate, and acrylates. ATRP method was successfully applied for preparation of resorcinarene centred stars bearing amphiphilic block copolymer arms [22].

Despite of the well known and investigated feature of calix[*n*]arenes to form complexes, the effect of the chemical composition and architecture of amphiphilic polymers bearing such macrocycles on the mechanism of the complex formation has not been well

* Corresponding author. Tel.: +358 9 19150333; fax: +358 9 19150330.
E-mail addresses: avt@hq.macro.ru (A.V. Tenkovtsev), Vladimir.Aseyev@helsinki.fi (V. Aseyev), Heikki.Tenhu@helsinki.fi (H. Tenhu).

0032-3861/$ – see front matter © 2010 Elsevier Ltd. All rights reserved.
doi:10.1016/j.polymer.2010.04.062

reported. Therefore, we intentionally designed two chemically similar but architecturally different star-shaped polymers with calix[8]arene core and neutral amphiphilic block copolymers as arms. The stars were synthesized using the arm-first approach. The star denoted herein as **4a** has arms with hydrophilic oligoethylene oxide block attached to the calix[8]arene core and alkyl outer block, whereas the other star denoted as **4b** has arms with inverse order of the blocks in respect to the core. Keeping in mind that oligoethylene oxide structures are widely used as podands for metal ions and the well known ability of calixarene to form complexes with different ionic and neutral species we believe that the combination of these moieties in one star-shape structure has allowed us to synthesise novel effective host molecules. Additionally it is possible to suppose that hydrophobic interactions in amphiphilic arms will prevent the ion release from the complex that obviously should increase the complexation ability of such polymers.

In this paper we report the complex formation between a series of metal ions and the star-block copolymers in respect to their macromolecular architecture. The ability of these polymers to extract cations from aqueous into organic phase is also presented. The observed difference in the extraction ability of the **4a** and **4b** stars is a consequence of their solubility and self-organization. Thus, in organic solvents these polymers form true, molecularly dispersed solutions with easily accessible calix[8]arene core, whereas multimolecular clusters are formed in aqueous media. The structure of these clusters depends on the order, in which the hydrophilic and hydrophobic blocks of the arms are attached to the calix[8]arene core. And this structure determines the accessibility of the macrocycles by the cations in water and hence the extraction ability of the **4a** and **4b** stars from aqueous into organic phase.

2. Experimental

2.1. Materials

Octa-t-butylcalix[8]arene was synthesized according to the earlier reported procedure [23]. All chemicals were purchased from Aldrich. Methylbromoacetate, sodium iodide, potassium carbonate, 11-bromoundecanoic acid, α-cetyl-ω-hydroxyoligoethylene oxide (M_w = 1000 g/mol, Brij-58) and ω-methyloligoethylene oxide (M_w = 1000 g/mol) were used as received, whereas thionyl chloride as well as solvents were purified by distillation. Alkali metal picrates were prepared from appropriate chlorides and sodium picrate (Aldrich) and twice recrystallized from water, while alkali metal chlorides as well as europium trichloride and uranyl nitrate (all p.a.) were used without additional purification. Dichloromethane was purchased from Vekton (Russia) and distilled before use. Aqueous solutions were prepared using deionised water from the Elgastat UHQ-PS water purification system.

2.2. 5,11,17,23,29,35,41,47-Octa-tert-butyl-9,50,51,52,53,54,55,56-octakis(carbomethoxy)calix[8]arene octamethyl ester ***(1a)***

A mixture of dried sodium iodide (3 g, 20 mmol) and methylchloroacetate (2 g, 18 mmol in dry acetone (50 ml) was stirred during 20 min and NaCl was filtered off. Potassium carbonate (5 g, 36 mmol) and *tert*-butylcalix[8]arene (1.3 g, 1 mmol) were added to a stirred filtrate as a dispersion in 100 ml of acetone. Reaction mixture was heated under reflux for 6 h, and was filtered after cooling. Evaporation of the solvent furnished a yellow solid that was recrystallized from ethanol. Yield was 1.4 g (77%) m.p. 239–240 °C ^{1}H NMR ($CDCl_3$) 1.10 (s, 72H), 3.52 (s, 24H), 4.05 (s, 16H), 4.07 (s, 16H), 6.97 (s, 16H).

2.3. 5,11,17,23,29,35,41,47-Octa-tert-butyl-9,50,51,52,53,54,55,56-octakis(carboxymethoxy)calix[8]arene ***(2a)***

A mixture of 0.9 g (0.48 mmol) **1** and 30 ml of 5% NaOH (ethanol/water 1/1 v/v solution) was stirred under reflux for 2 h. After acidification, the product was filtered off and twice recrystallized from methanol. Yield was 0.63 g (74%) m.p. 239–240 °C ^{1}H NMR ($CDCl_3$) 1.10 (s, 72H), 3.5 (s, 24H) 4.07 (s, 16H), 6.92 (s, 16H).

2.4. 5,11,17,23,29,35,41,47-Octa-tert-butyl-9,50,51,52,53,54,55,56-octakis(chlorocarbonyloxymethoxy)calix[8]arene ***(3a)***

A suspension of **2** (0.42 g, 0.24 mmol) in a mixture of $SOCl_2$ (5 ml) and benzene (20 ml) was stirred under reflux for 2 h. After the solvent evaporation, slightly yellow powder was recrystallized from hexane. Yield was 0.32 g (71%) m.p. 150–152 °C ^{1}H NMR ($CDCl_3$) 1.17 (s, 72H), 3.5 (s, 24H) 4.72 (s, 16H), 6.92 (s, 16H).

2.5. 5,11,17,23,29,35,41,47-Octa-tert-butyl-9,50,51,52,53,54,55,56-octakis(carboxymethoxy)calix[8]arene octa(eicosaethylene glycol hexadecyl ether) ester ***(4a)***

A solution of **3** (0.27 g, 0.14 mmol) and Brij-58 (1.27 g, 1.13 mmol) in 2 ml of dodecane was heated at 180 °C during 2 h under the argon atmosphere. After cooling, the solvent was evaporated in vacuum and polymer was reprecipitated twice from methylene chloride (1 ml) to hexane (50 ml) and dried (50 °C, 0.1 torr). Yield was 1.1 g (84%) ^{1}H NMR ($CDCl_3$) 0.88 (s, CH_3), 1.23–1.36 (m, CH_2), 3.36–3.51 (m, OCH_2CH_2O) 4.29 (t, OCH_2), 6.92 (s, Ar-H).

2.6. 5,11,17,23,29,35,41,47-Octa-tert-butyl-9,50,51,52,53,54,55,56-octakis(10′-carbodecyloxy)calix[8]arene octaethyl ester ***(1b)***

A mixture of 1.94 g (5.95 mmol) Cs_2CO_3, 0.77 g (0.59 mmol) of *tert*-butylcalix[8]arene and 4.12 g (11.8 mmol) of ethyl 11-iodoundecanoate [24] in 50 ml of acetone was heated under reflux for 72 h. After cooling cesium salts were filtered off and filtrate poured into 100 ml of water. Crude product was recrystallized from ethanol–-chlorophorm (1/2 v/v) mixture. Yield was 1.4 g (79%) ^{1}H NMR ($CDCl_3$) 1.04 (s, 72H), 1.4 (m, 128H), 1.65 (t, 24H) 2.29 (t, 16H) 3.61 (t, 16H), 4.05 (s, 16H), 4.13 (*q*, 16H), 6.92 (s, 16H).

2.7. 5,11,17,23,29,35,41,47-Octa-tert-butyl-9,50,51,52,53,54,55,56-octakis(10′-carboxydecyloxy)calix[8]arene ***(2b)***

A mixture of 1 g (0.33 mmol) **1b** and 20 ml of 5% NaOH (ethanol/water 1/1 v/v solution) was stirred under reflux for 2 h. After acidification, the product was filtered off and twice recrystallized from methanol. Yield was 0.77 g (85%) ^{1}H NMR ($CDCl_3$) 1.22 (s, 72H), 1.4 (m, 128H), 2.30 (t 16H), 3.51 (t, 16H), 4.11 (s, 16H) 6.92 (s, 16H).

2.8. 5,11,17,23,29,35,41,47-Octa-tert-butyl-9,50,51,52,53,54,55,56-octakis(10′-chlorocarbonyldecyloxy)calix[8]arene ***(3b)***

A suspension of **2b** (0.39 g, 0.14 mmol) in a mixture of $SOCl_2$ (1.5 ml) and benzene (4 ml) was stirred under reflux for 8 h. After the solvent evaporation, white powder was recrystallized from hexane. Yield was 0.28 g (71%) ^{1}H NMR ($CDCl_3$) 1.21 (s, 72H), 1.4 (m, 128H), 2.33 (t 16H), 3,51 (t, 16H), 4.15 (s, 16H) 6.94 (s, 16H).

2.9. 5,11,17,23,29,35,41,47-Octa-tert-butyl-9,50,51,52,53,54,55,56-octakis(10′-chlorocarbonyldecyloxy)calix[8]arene octa (polyethleneglycol-1000 ω-methyl ether) ester (4b)

A solution of **3b** (0.2882 g, 0.0988 mmol) and PEG1000-ω-methyl ether (0, 7912 g, 0.79 mmol) in 2 ml of dodecane was heated at 180 °C during 2 h under the argon atmosphere. After cooling, the solvent was evaporated in vacuum and polymer was reprecipitated twice from methylene chloride (1 ml) to diethyl ether (50 ml) and dried (50 °C, 0.1 torr). Yield was 0.8 g (74%) ^{1}H NMR ($CDCl_3$) 1.29 (s, $(CH_3)_3C$), 1.12–1.74 (m, CH_2), 2.33 (t CH_2COO), 3.39 (s, OCH_3), 3.36–3.71 (m, OCH_2CH_2O), 4.23 (t, OCH_2), 6.93 (s, Ar-H).

2.10. Binding constant measurements

Methanol (Vecton, RF) was used as a solvent without additional purification. The changes in the UV spectra were recorded from 250 to 300 nm for the series of the polymer solutions in methanol upon stepwise increasing the metal cation concentration. The concentration of the polymers (i.e., the molar concentration of calixarene rings) was 1×10^{-4} M, while the concentration of metal salt varied from 0 to 1×10^{-3} M. The cations were introduced as chlorides or as nitrate in the case of uranyl (all p.a.). Samples were stored at room temperature for about 12 h prior the measurements to reach equilibrium complex formation. After this period no changes in the UV spectra have been detected. Also no influence of the NO_3^- ions on the spectra of the uranyl containing solutions was observed. Stoichiometries of complexes were determined by the method of continuous variation using the deviation from Beer's law in the UV spectra at 278 nm for the series of mixtures of polymer and inorganic salts in methanol (so called Job's plot) [25]. In all these cases the total concentration of polymer and inorganics was 1×10^{-4} M.

2.11. Extraction measurements

Extraction measurements were performed in a dichloromethane/water composition with 1:1 volume ratio of the combined solutions. The extracting polymers and extracted picrates were dissolved separately: the picrates were dissolved in water, whereas solutions of the star polymers **4a** and **4b** as well as the calixarene derivative **2a** were prepared in dichloromethane. The molar concentration of the picrates and the functional groups of the polymers was the same, i.e., 1.35×10^{-4} mol/l. The freshly made solutions were left overnight to insure entire solubilisation. Solutions of polymers in dichloromethane (5 ml) and aqueous solutions of picrates (5 ml) were mixed, vigorously shaken for 3 min, and obtained emulsions were kept steady until complete liquid–liquid macro phase separation. The concentration of the picrate ions extracted by the polymers into the organic phase was determined spectrophotometrically using the absorption measurements at 355 nm, the longest wavelength adsorbtion maximum of Bu_4N^+ picrate in CH_2Cl_2 that was used as a reference compound prepared in situ from picric acid and $Bu_4N^+OH^-$.

2.12. Instrumentation

^{1}H NMR spectra were recorded on a Bruker DRX 400 NMR spectrometer operating at 400.13 MHz for ^{1}H. UV measurements were recorded on a Cary 100 Varian spectrophotometer. Dynamic (DLS) and static (SLS) light scattering measurements were conducted using a Brookhaven Instruments BI-200SM goniometer, a BIC-TurboCorr digital crosscorrelator, and a BI-CrossCorr detector, including two BIC-DS1 detectors. A helium–neon Spectra Physics laser operating at the wavelength of $\lambda_o = 632.8$ nm and a Sapphire 488-100 CDRH laser from Coherent GmbH operating at $\lambda_o = 488$ nm and the power adjusting from 10 to 50 mW were used as light sources. Scattered light was collected between $\theta = 30°$ and $\theta = 150°$ scattering angles. Time-correlation functions were analyzed with an inverse Laplace transform program CONTIN (BIC software). Mean peak value of a size distribution was a matter of choice to estimate an apparent hydrodynamic radius of scattering objects, R_h. 3–5 correlation curves with various accumulation times were collected for each sample to check the reliability of the mathematical solution provided by CONTIN. The time average intensity of the scattered light, I_θ, was recorded simultaneously with correlation functions and the intensities measured in counts of photons per second, cps, were normalised with respect to the Rayleigh ratio of toluene. Constant intensity of the light scattered at 90° angle was used as a criterion of the solution equilibrium. Aqueous solutions were passed through the hydrophilic Millex-HV 0.45 μm pore size and 13 mm in diameter filters prior to measurements, to remove dust particles. The temperature of the samples was controlled by means of a Lauda RC 6C thermostat. Wyatt Optilab rEX differential refractometer ($\lambda_o = 632.8$ nm) was used to determine the specific refractive index increment, dn/dc_p. Within the experimental error $dn/dc_p = 0.146$ mL/g for both **4a** and **4b**. All the studies were performed at 20 °C.

3. Results and discussion

3.1. Synthesis and characterization

The synthetic approach to designed star polymers is presented in Scheme 1. We have used traditional synthetic procedures keeping in mind that availability of the well-defined oligoethylene oxides and other hydroxyl-terminated oligomers gives the possibility to vary the arm chemical structure when needed. Success in the polymer synthesis using a condensation approach was ascertained by a proper choice of the esterification procedure. Complete substitution of the reactive groups of a multifunctional monomer is one of the most essential problems in the dendrimer chemistry [26]. The same challenge was encountered during the synthesis of the star polymers under investigation. A typical approach to

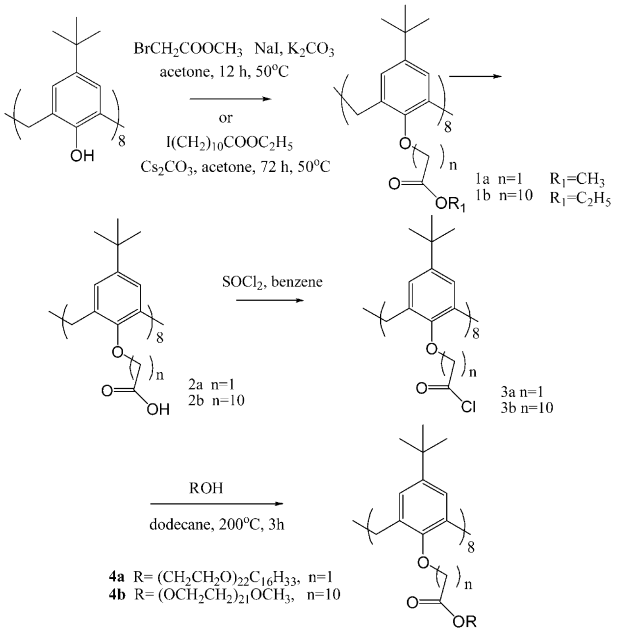

Scheme 1. The synthetic route to the star polymers.

overcome this difficulty is to use an excess of the monofunctional monomer under conditions that are usual for an esterification according Einhorn method (e.g., use of pyridine or $(C_2H_5)_3N$ as catalyst and HCl acceptor). Unfortunately our attempt to synthesize **4a** and **4b** in this way showed that the isolation of the polymer is problematic owing to the high solubility of both the ester and the precursor, either in water or in organic solvents. On the other hand, heating of the reactants of near the equimolar ratio at 180–200 °C in inert solvent like diphenyl oxide, hexadecane etc. gave the designed product in a high yield while the purity of the product was about 98% (UV data).

The number and polydispersity of the arms of the star polymers prepared using the core-first synthesis is typically determined by selective detaching the arms. However, for the polymers discussed herein the molecular weight and PDI of the presynthesized arms are 1100 g/mol and $M_w/M_n = 1.1$, respectively according to Aldrich. Due to the relatively low molecular weight, the quantitative NMR analysis as well as UV spectroscopy can easily be applied to determine the content of the aromatic moieties and thus the true arm number. From a comparison of the absorption of the polymer solution in ethanol at 280 nm (absorption maximum of the calixarene core) with the absorption of the model compound (**2a**), the actual average number of the arms is about 7.6–7.8, while the NMR data gives 7.2–7.7 for **4a** and **4b**.

3.2. Binding ability of polymer towards metal ions in methanol

4a and **4b** are well soluble in several organic solvents and according to our light scattering data form molecularly dispersed solutions in toluene, dichloromethane and methanol. In water these polymers form multimolecular aggregates and their binding ability cannot be measured accurately. Hence, ionophoric properties of star polymers were investigated in methanol using alkaline metal chlorides (Li–Na–K–Rb–Cs) as well as europium chloride and uranyl nitrate. The choice of methanol is based on the fact that the polymers form real solutions in this rather polar solvent and therefore methanol is used as a reference solvent in further discussion on the extraction experiments in water/dichloromethane system. The selected cations have a tendency to form complexes with "oxygen"-type ligands (e.g., carbonyl and ester type ligands). Methanol solutions of the selected metal salts were added to the methanol solutions of polymers.

The process of the complex formation between the star polymers and the metal cations has been followed by monitoring the increase in the absorption at about 270–280 nm, which is characteristic to the $\pi-\pi^*$ transition in substituted benzene, see Fig. 1. Such a change in the absorption spectrum is likely related to the formation of a polymer/cation complex, in which the bound cation is closely located to the calixarene cores, as has been shown for the model compound **2a** [27]. Molecular composition of the complex has been determined by the method of continuous variation [25], see the Job's plot in Fig. 2. In accordance with this method, an addition of the methanol solution of the selected metal chloride into the star polymers solution results in increasing absorption at 276 nm, which is used to determine the polymer/metal cation ratio in the complex.

Our experiments reveal that, Li^+, Na^+, Eu^{3+} chlorides do not form complexes with stars **4a** and **4b**. In contrast, **4a** and **4b** both form 1:2 complexes with K^+ and Rb^+, while these polymers form 1:1 complexes with Cs^+ and 2:1 complexes with UO_2^{++}. This well correlates with the ionic size of the studied cations and also corresponds to the earlier reported data [28] on the complementarity of Cs^+ and calix[8]arene molecule.

The average (geometric mean of the first and the second association constants in the case of 1:2 and 2:1 complexes) binding

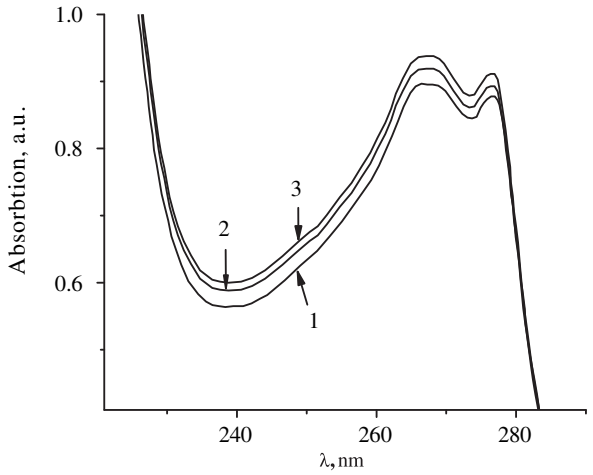

Fig. 1. UV spectra of the **4a** solution in methanol with varying the molar ratio of cesium chloride and **4a**: CsCl/**4a** = 0 (1) 1 (2) 100 (3).

constants of the complexes have been estimated photometrically using the mole ratio method [29], see Table 1. It is evident that the binding properties of the complexes increase in a sequence $K^+ < Rb^+ < Cs^+$, which presumably is associated with the increasing the ionic size and the coordination number of the cations in that sequence.

One should note that the binding constants of the studied complexes formed between the star polymers and the alkali metal chlorides are comparable with the constants reported for the complexes of these cations with dibenzo-18-crown-6 in the same solvent, i.e., lg $\beta = 5.0$ for K^+, 4.2 for Rb^+, and 3.5 for Cs^+ [30]. Dibenzo-18-crown-6 is a typical representative of the class of crown ethers. However, an inverse dependence of the complex stability upon the ionic radius of cation was observed for star **4a**. The latter may be a result of bigger size of the calix[8]arene cycle compared to that of dibenzo-18-crown-6.

3.3. Extraction of picrates from water into dichloromethane

Ionophoric properties of the star polymers have also been investigated using extraction of picrates of alkali metals from water into the solution of the stars in dichloromethane. This method has successfully been applied for the semi quantitative analysis of ionophoric properties (phase-transfer ability in CH_2Cl_2/H_2O system

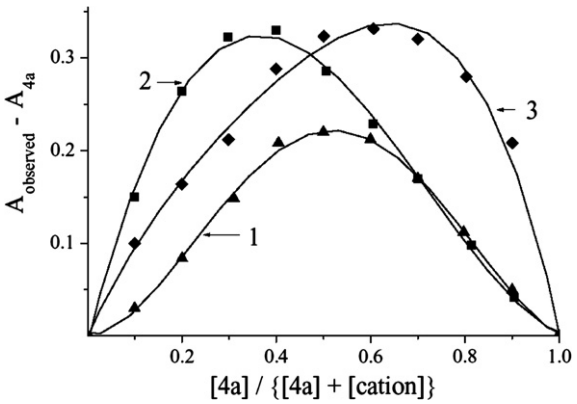

Fig. 2. The Job's plots for the **4a** solution in methanol with varying the molar ratio of metal chloride and **4a**: CsCl (1) RbCl (2) $UO_2(NO_3)_2$ (3). The total concentration of [**4a**] + [metal salt] is 1×10^{-4} M.

Table 1
The average binding constants of the complexes under investigation. Methanol, 25 °C.

Polymer	Cation	Complex composition (polymer to metal ratio)	Average binding constant, lg β
4a	K^+	1:2	4.53
	Rb^+	1:2	5.07
	Cs^+	1:1	5.13
	UO_2^{++}	2:1	4.61
4b	K^+	1:2	2.97
	Rb^+	1:2	5.07
	Cs^+	1:1	5.44
	UO_2^{++}	2:1	4.65

in comparison with binding constants to alkali metals in methanol solution) of the lower mass calixarenes [2]. It was shown that percentage of extraction of the metal picrates into CH_2Cl_2 correlate with stability constants. It was of interest to investigate such correlations in the case of star-shaped polymers with the same core moiety keeping in mind the abovementioned colloidal nature of polymer solution in water and amphiphilic arms with oligoethylenoxide fragments that can also act as ligands and phase-transfer catalysts.

In our studies, concentrations of picrate ions in organic phase were determined spectrophotometrically at the wavelength of 355 nm. Our blank experiments show that (1) the distribution coefficients of **4a** and **4b** in CH_2Cl_2/H_2O system are 0.89 and 0.82 respectively and (2) picrates are insoluble in dichloromethane in the absence of star polymers (concentration of the saturated picrates solution is below 10^{-7} M) and do not transfer from the aqueous into organic phase. However, picrates are detected in the organic phase in the presence of the star polymers and their concentration can be measured using Bu_4N^+ picrate as the reference compound. In our opinion indirect UV determination of ions in the organic phase from the rest of picrate in water is less accurate due to the presence of colloidal particles.

Table 2 demonstrates that **4a** is a better extracting agent in comparison with its low molar mass analog **2a**. Herewith, the effectiveness of the extraction increases with increasing the ionic radius of the cation and correlates with the increase in the corresponding binding constants. One may suggest that the higher extraction capability of the polymer **4a** in comparison with its low molar mass analog **2a** arises from the oligoethylene oxide arms, which is widely used as a podand for alkaline metals [31]. However, the extraction ability of ω-cetyl oligoethylene oxide (Brij-58) solutions in respect to cations of alkali metals is significantly lower than that of the polymer **4a**. Therefore, we conclude that the formation of the star **4a**/metal cation complex is primarily determined by the interaction of the cation with the ester groups, which are directly bound to the calix[8]arene macrocycle.

It is interesting to compare the phase-transfer ability of **4a** toward metal ions with the well documented transport properties

Table 2
Percent of extraction of the metal picrate into CH_2Cl_2 at 20 °C.

Phase-transfer catalyst	Percent of extraction of alkali metal Picrate		
	KCl	RbCl	CsCl
4a	26.3	37.3	50.6
4b	14.7	4.6	3.6
2a (model compound)	25.5	29.6	20.1
ω-cetyloligoethyleneoxide (Brij-58)	1.2	1.5	1.5

of usual crown ethers [32]. It was found that the extraction ability of crown ethers toward a definite alkali metal ion strongly depends on the macrocycle size. The distribution coefficient usually achieves the highest value for potassium picrate and decreases for cesium and sodium ones. For example, percent of extraction of alkali metal picrate in $CHCl_3/H_2O$ system in the presence of 18-crown-6 decreases in a sequence $K^+ > Rb^+ > Cs^+ > Na^+$ and drops to one half moving from potassium (68%) to cesium (31%) [33]. In the case of **4a**, the extraction ability is the highest toward cesium picrate owing to complementarity of Cs^+ and calix[8]arene molecule [28] and twice lower than that for potassium salt.

One may expect that the star with an inverse sequence of the hydrophobic-hydrophilic blocks (**4b**) demonstrates nearly the same phase-transfer ability. Surprisingly, the ionophoric property of **4b** is significantly lower than that of the model compound **2** and its isomer **4a.** In addition, the star **4b** reveals an inverse dependence between the amount of extracted picrate and the corresponding binding constant, see Fig. 3. Thus, the molecular architecture evidently affects the extraction capability and probably strongly depends on the structure of polymer clusters in water solution.

3.4. Light scattering measurements of aqueous solutions

The observed difference in the extraction ability of the **4a** and **4b** stars is a consequence of their solubility and self-organization. Dichloromethane is a thermodynamically good solvent for these polymers, which form molecularly dispersed solutions. Water is not as good solvent as CH_2Cl_2 and multimolecular clusters are formed in water due to the hydrophobic interaction between the stars. However, the structures of the clusters formed by the **4a** and **4b** stars are expected to be different and defined by the order, in which the hydrophilic and hydrophobic blocks of the arms are attached to the calix[8]arene core. Depending on the self-organization of stars in water, the hosting calix[8]arene core is either more or less accessible for the cations, which defines capture and transfer of the cations in organic phase. Therefore, we performed dynamic, DLS, and static, SLS, light scattering studies of aqueous solutions of stars in order to find a correlation between their molecular architecture, self-assembling, cation binding ability and ionophoric properties.

Light scattering from aqueous solution of the **4a** star was studied using the wavelength of λ_o = 632.8 nm and the **4b** star of λ_o = 488 nm. A narrow band interference filter was used in front of the detector. At these wavelengths, no fluorescence was detected but at a concentration higher than 10 g/l the intensity of the

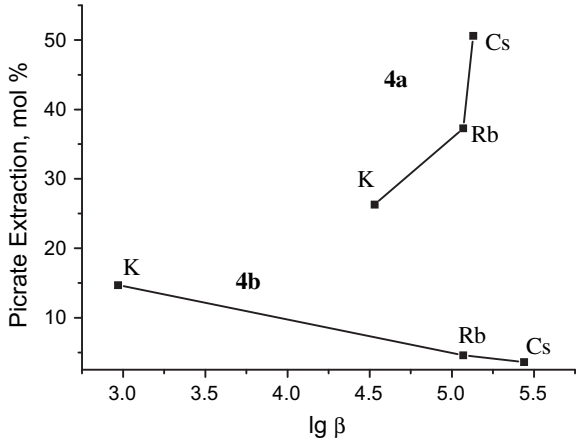

Fig. 3. Dependence of the polymer extraction ability vs. binding constants of the polymers toward alkali metal ions.

scattered light was strong presumably because of the Tyndall effect. Due to this, one may expect that these star-shaped polymers form multimolecular aggregates/clusters in water.

In the DLS experiments, the translational diffusion coefficient, $D = \Gamma q^{-2}$, actually is measured rather than the hydrodynamic radius, $R_h = kT/(6\pi\eta_o D)$, where the scattering wave vector is $q = (4\pi n_o/\lambda_o)\sin(\theta/2)$, n_o is the refractive index of solvent, η_o is the solvent viscosity, $\Gamma = 1/\tau$ is the decay rate. The measured D (and thus R_h) is apparent and concentration dependent. For monodisperse spherical particles the true value of the hydrodynamic radius is obtained at zero scattering angle, θ, and at infinite dilution.

For both **4a** and **4b** star polymers, distributions of the apparent hydrodynamic radius are monomodal within the studied range of the polymer concentrations. The mean hydrodynamic radius, R_h, does not depend on the way, in which the solutions have been prepared, i.e., either by dilution of the stock solution or by direct preparation the solution with the predefined polymer concentration, c_p. Dependence of the decay rate Γ_1 (calculated using the 2nd order cumulant analysis) vs. scattering vector q^2 passes through the centre of coordinates thus representing a diffusive process. In the range of large q, Γ_1 vs. q^2 deviates up from linearity and in combination with a weak angular dependence of R_h (calculated using CONTIN) suggests a moderate polydispersity of the scattering particles. Therefore, the extrapolation of R_h to zero angle primarily describes the fraction of large scatterers. The radius of gyration, R_g, was estimated using the initial slope of the q^2 vs. LS intensity and thus describes the same large particles.

Dilution typically decreases the aggregation number or even disintegrates multimolecular clusters completely. However, the latter was not observed for either of the polymers. Thus for **4b** star, the size of the aggregates is nearly the same below $c_p = 0.1$ g/L Fig. 4 suggests that the mass weighted molar mass of the clusters formed by the **4b** star at infinite dilutions, $M_w = [Kc_p/(I - I_o)_{\theta=0^\circ}]^{-1}$, is about 20×10^6 g/mol. This gives the aggregation number in a cluster of about 2000 **4b** molecules. Under the same condition, R_h is 108 nm and R_g is 70 nm, see Fig. 5. Below $c_p = 0.1$ g/L, size of the clusters does not depend on the way, how the solution was prepared, which suggests equilibrium character of the system. Assuming a uniform distribution of the polymeric material within the clusters we estimated the packing density of polymeric material, which equals the clusters overlap concentration $c_p^* = M_w/[N_A 4/3\pi R_h^3]$ of about 6 g/L. Therefore, the concentration region of $c_p < 0.1$ g/L definitely corresponds to dilute solutions.

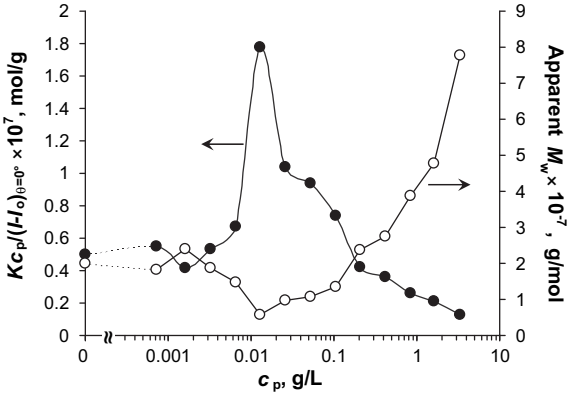

Fig. 4. Dependence of the inverse reduced intensity of the scattered light $Kc_p/(I - I_o)_{\theta=0^\circ}$ (●) and the apparent molar mass M_w (○) on the concentration of the **4b** star, c_p. Here, K is the optical constant, I and I_o are the intensities of light scattered by solution and by solvent respectively. By taking the average of the intensities measured for the three most dilute polymer solutions, we assume absence of any interactions between the particles and get a value close to that extrapolated to zero c_p.

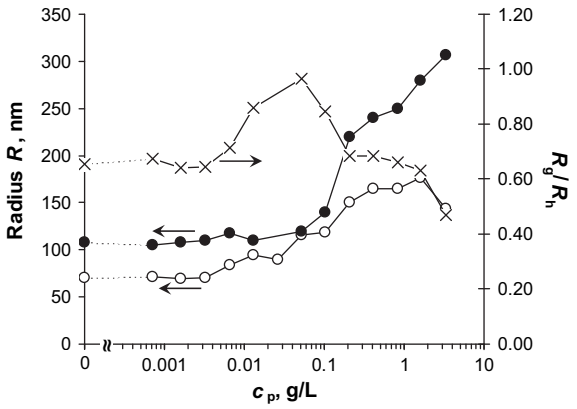

Fig. 5. Dependencies of the apparent hydrodynamic radius R_h (●), of the radius of gyration R_g (○), and the shape parameter R_g/R_h (×) on the concentration of the **4b** star, c_p. By taking the average of the radii measured for the three most dilute polymer solutions, we assume to get a value close to that at zero c_p.

For **4a** star, size of the aggregates is nearly the same in a wide range of the concentrations studied though one can notice a small change in the slope of the R_h vs. c_p dependence around $c_p = 2$ g/l, see Fig. 6. The angular dependence of intensity of the scattered light reveals no significant effect of c_p on the radius of gyration, R_g, of the aggregates in dilute solutions of **4a** star. For example, for solutions of $c_p = 0.33$ and 3.62 g/l, dimensions of the scatterers are $R_g = 108$ and 110 nm and $R_h = 117$ and 120 nm respectively. Furthermore, the critical aggregation concentration (if such actually exists) is found to be lower than $c_p = 0.013$ g/l (the lowest concentration studied). The mass of the **4a** aggregates was $M_w = 12 \times 10^6$ g/mol and thus the association number was 1200 and $c_p^* = 1$ g/l for the clusters of $R_h = 120$ nm. The latter suggests that the changes in the line slopes in Figs. 6 and 7 originate from the crossover concentration of the aggregates.

The overlap concentration was also tested using viscosimetric measurements, Fig. 7. The c_p^* values are naturally higher than those determined using light scattering due to the shear thinning effect. In addition, flow destroys the clusters and the measured intrinsic viscosities correspond to the individual molecules. Decrease in R_h upon dilution of **4a** below c_p^* in the absence of flow (Figs. 5 and 6) evidently originates from the hydrodynamic interactions. At much lower concentrations, i.e., $c_p < 0.1$ g/L, hydrodynamic interactions between the clusters practically disappear and R_h does not depend on c_p (Fig. 5). One can also note that the second virial coefficient, A_2,

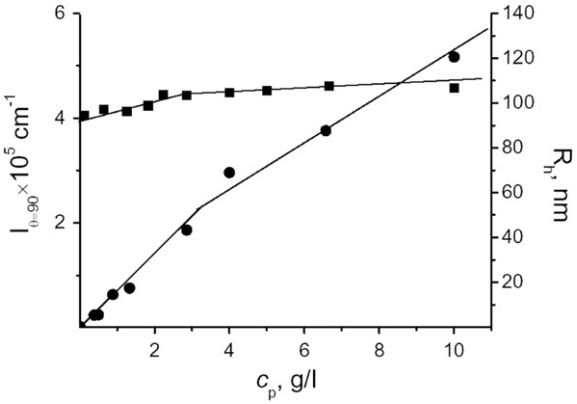

Fig. 6. The apparent hydrodynamic radius (■), R_h, and the scattered light intensity (●), I, versus the concentration c_p of aqueous **4a**, obtained at the scattering angle of $\theta = 90^\circ$.

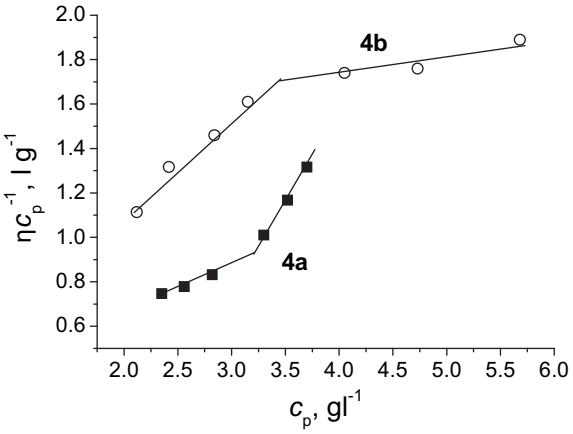

Fig. 7. Concentration dependence of the reduced viscosity of aqueous **4a** and **4b**.

is about zero below $c_p < 0.1$ g/L: hydrophobic moieties and high molar mass of the aggregates decrease solubility of the stars in respect to highly soluble PEO, especially if one takes into account that the weight content of the hydrophobic moieties is about twice higher than that of the hydrophilic ones. At higher concentrations A_2 becomes positive owing to the strong intermolecular interactions in semidilute solutions. However, change in the slope of the viscosity vs. c_p curves obtained for **4a** and **4b** are different and reveal dissimilar processes in vicinity of c_p^* when *inter* cluster interactions compete with *intra* cluster interactions. This dissimilarity clearly originates from the polymer architecture.

What might be the architecture of the multimolecular aggregates of the star polymers? Let's assume that an aggregate has a structure of a spherical micelle. Then its radius should be of the order of one length of a fully stretched star arm, which is about 25 nm from the known degree of polymerization. On the other hand, rough molecular mechanics calculation (MM+, HyperChem package 7.0) gives diameter of **4a** of about 10 nm that is more reasonable because the arms are coiled. This value is significantly smaller than the experimentally measured R_h of 117 nm (for $c_p = 0.33$ g/l) and therefore the model of a spherical micelle does not fit our experimental data. Not strongly pronounced change in the slope of the concentration dependence of the scattered light intensity at about $c_p = 3$ g/l coincides with the slope change in the R_h vs. c_p dependence and seems to reflect a solution restructuring. Thus a decrease in the slope of the $I_{\theta=90}$ vs. c_p dependence upon increasing c_p may occur when the scattering particles overlap reducing the amount of concentration fluctuations. Taking into account the large size of the aggregates, we assume that the kink is related to the crossover concentration, c_p^*.

The crossover concentration numerically coincides with the density of polymeric material within the aggregates and signifies that the aggregates are not dense. The shape parameter for the **4b** star $R_g/R_h = 0.65$, which suggests that particles are denser in vicinity of the centre of gravity. This is well expected for association of molecules with hydrophobic blocks. In contrast, $R_g/R_h = 0.92$ for the **4a** star. This value is higher than 0.78 for a hard sphere but smaller than 1.5 for a solvent draining Gaussian coil [34] and may describe solvent draining particles with uniform (i.e., non-Gaussian) distribution of polymeric material within it. The aliphatic blocks at the end of each arm are hydrophobic and likely to associate either with each other or with the calixarene. One may anticipate the formation of supramolecular assemblies, where entanglements between individual stars are formed by the loops of the arms. Taking into account the polydispersity of the scattering particles, these R_g/R_h values are not absolute ones but rather estimative values. Unfortunately, the aggregates are not large enough to resolve their fine structure with a Kratky plot [35] using red light as a source of the incident radiation.

4. Conclusions

Amphiphilic star-shaped copolymers with a calixarene core have been studied as polymeric hosts for metal ions and their ionophoric properties towards alkaline metal, lanthanide and uranyl ions were investigated. Either of the star copolymers **4a** and **4b** form molecularly dispersed solution in organic solvents. However, multimolecular aggregates with complex morphology are formed in water. It was found that the ability of the star polymers to bind selected cations in water drastically depend on the sequence of the hydrophilic and hydrophobic blocks in the arm. As a result, also the ability of these stars to transfer cations from aqueous into organic phase depends on the order in which the oligoethylene oxide and the alkyl blocks are connected to the calixarene core. Thus, the **4a** star that has the (hydrophobic core) → (hydrophilic block) → (hydrophobic block) sequence of structural elements form aggregates with the aggregation number of about 1200 and the shape factor $R_g/R_h \approx 0.92$ in water. Although this value is close to 0.78 for a hard sphere, we suppose that the multimolecular assemblies of stars are solvent draining and the average density of polymeric material within an aggregate is of the order of $c_p^* = 2–3$ g/l. The aliphatic blocks at the end of each arm are randomly associated either with each other or with the calixarene. Loops of the arms may form additional entanglements of a locked ring type between individual stars and thus increase density of the aggregates. The **4b** stars with (hydrophobic core) → (hydrophobic block) → (hydrophilic block) sequence of structural elements form aggregates of about 2000 units and shape factor $R_g/R_h = 0.65$. One can assume that in this case the micogel forms inside the particle due to the interactions between calixarene-undecyl moieties that leads to less accessibility of the binding sites near macrocyle for cations and therefore the lower phase-transfer efficiency of **4b** in comparison to **4a**.

As has been demonstrated, the effectiveness of these star-shaped block copolymers as phase-transfer agents seems to be strongly regulated by their supramolecular organization in water. We conclude that in organic solvents the binding properties of **4a** and **4b** preferably depend on the presence of calixarene moiety in the polymer structure and in a smaller degree on noncovalent interaction of cations with the functional groups of arms. On the other hand, the supramolecular assembling in water determines the access of the cations to the calixarene binding sites. The more detailed investigation of the aggregates structure is in progress.

Acknowledgements

Authors are thankful to the Academy of Finland (grant no. 118566) and to the Russian Foundation for Fundamental research (grant no. 07-03-91000a) for the financial support.

References

[1] Whittaker MR, Monteiro MJ. Langmuir 2006;22(23):9746–52.
[2] Miao JJ, Xu GQ, Zhu L, Tian L, Uhrich KE, Avilia-Orta CA, et al. Macromolecules 2005;38(16):7074–82.
[3] Sheng YJ, Nung CH, Tsao HK. J Phys Chem B 2006;110(43):21643–50.
[4] Podoprygorina G, Zhang J, Brusko V, Bolte M, Janshoff A, Boehmer V. Org Lett 2003;5(26):5071–4.
[5] Yang Y, Swager TM. Macromolecules 2006;39(6):2013–5.
[6] Liu Y, Li L, Fan Z, Zhang HY, Wu X, Guan XD, et al. Nano Lett 2002;2(4):257–61.

[7] Gutsche CD, Dhawan B, Na KH, Muthukrishnan R. J Am Chem Soc 1981;103 (13):3782–92.
[8] Danil de Namor AF, Cleverley RM, Zapata-Ormahea ML. Chem Rev 1998;98 (7):2495–526.
[9] Krause T, Gruner M, Kuckling D, Habicher WD. Tetrahedron Lett 2004;45 (52):9635–9.
[10] Uhrich KE, Cannizzaro SM, Langer RS, Shakesheff KM. Chem Rev 1999;99 (11):3181–98.
[11] Quellet C, Schudel M, Ringgenberg R. Chimia 2001;55(5):421–8.
[12] Flor de María R, Charbonniere L, Muller G, Bünzli J-CG. Eur J Inorg Chem 2004;2004(11):2348–55.
[13] Kennedy JP, Jacob S. Acc Chem Res 1998;31(12):835–41.
[14] Hadjichristidis N, Pitsikalis M, Pispas S, Iatrou H. Chem Rev 2001;101 (12):3747–92.
[15] Taton D, Saule M, Logan J, Duran R, Hou S, Chaikof EL, et al. J Polym Sci: Polym Chem 2003;41(11):1669–776.
[16] Jacob S, Majoros I, Kennedy JP. Macromolecules 1996;29(27):8631–41.
[17] Shim JS, Kennedy JP. Polym Bull 2000;44(5–6):493–9.
[18] Ueda J, Kamigaito M, Sawamoto M. Macromolecules 1998;31(20):6762–8.
[19] Angot S, Murthy KS, Taton D, Gnanou Y. Macromolecules 1998;31 (21):7218–25.
[20] Angot S, Murthy KS, Taton D, Gnanou Y. Macromolecules 2000;33(20):7261–74.
[21] Gnanou Y, Taton D. Macromol Symp 2001;174(1):333–41.
[22] Strandman S, Luostarinen M, Niemela S, Rissanen K, Tenhu H. J Polym Sci: Polym Chem 2004;42(17):4189–201.
[23] Gutsche CD, Iqbal M. Org Synth 1989;68:234.
[24] Bergbreiter D, Whitesides G. J Org Chem 1975;40(6):779–82.
[25] Job P. Annali di Chimica Applicata 1928;9(2):113–203.
[26] Busson P, Ortegren J, Ihre H, Gedde UW, Hult A, Andersson G, et al. Macromolecules 2002;35(5):1663–71.
[27] Arnaud-Neu F, Collins EM, Deasy M, Ferguson G, Harris ASJ, Kaitner IB, et al. J Am Chem Soc 1989;111(23):8681–91.
[28] Otsuka H, Suzuki Y, Ikeda A, Araki K, Shinkai S. Tetrahedron 1998; 54(3–4):423–46.
[29] Beck M, Nagipal I. Chemistry of complex equilibria. Budapest, Hungary: Akademiai Kiado; 1989.
[30] Hofmanova A, Koryta J, Brezina M, Mittal M. Inorg Chim Acta 1978;28:73–6.
[31] Allcock HR, O'Connor SJM, Olmejer DL, Napierala ME, Cameron CG. Macromolecules 1996;29(23):7544–52.
[32] Linday LF. The chemistry of macrocyclic ligand complexes. Cambridge, UK: Cambridge University Press; 1990.
[33] Marchand AP, Chang HS. Tetrahedron 1999;55(32):3687–96.
[34] Burchard W. Adv Polym Sci 1999;143:113–94.
[35] Kratky O, Porod G. J Colloid Sci 1949;4(1):35–70.